Thermomechanical analysis of oscillatory pin-bushing performance

Rajesh Krithivasan* — Michael M. Khonsari**

** Product Engineer (R&D), Dresser Inc.*
LA Highway 3225 @ US-167N
Alexandria, LA-71309, United States of America
rkrithiv@consolidatedvalve.com

*** Dow Chemical Endowed Chair and Professor*
Department of Mechanical Engineering, Louisiana State University
Baton Rouge, LA-70803, United States of America
khonsari@me.lsu.edu

ABSTRACT. *This paper presents a Finite Element Analysis (FEA) to effectively describe the thermomechanical interactions of a heavily loaded oscillating pin-bushing pair used in earthmoving equipment. An objective of this analysis is to predict the time to failure when a pin-bushing pair is subjected to heavy loads and to improve performance and increase the Mean Time between Failures (MTBF). FEA results reveal that two types of failure can take place depending on different operating parameters. They are: (i) Thermally Induced Seizure and (ii) Scuffing. An extensive set of parametric simulations covering load, speed, shaft radius, operating clearance, bearing length, friction coefficient and thermal expansion coefficient are performed to gain insight into the failure of oscillating pin-bushings. A statistical procedure is applied to the simulated results and an empirical relationship is derived.*

RÉSUMÉ. *Cet article présente une analyse par éléments finis (FEA) pour décrire efficacement les interactions thermomécaniques d'un ensemble pion-disque fortement chargé soumis à des oscillations et utilisé dans des équipements de terrassement. Un objectif de cette analyse est de prévoir la durée de fonctionnement d'un ensemble pion-disque fortement chargé, d'améliorer les performances et d'augmenter le temps moyen entre les échecs (moyenne des temps de bon fonctionnement). Les résultats obtenus par FEA indiquent que deux types d'échec peuvent avoir lieu selon différents paramètres de fonctionnement : 1) attaque thermiquement induite et 2) éraillure. Un ensemble de simulations paramétriques couvrant la charge, la vitesse, le rayon, le jeu de fonctionnement, la longueur, le coefficient de frottement et le coefficient de dilatation thermique sont effectuées pour améliorer le fonctionnement d'un ensemble pion-disque en régime oscillatoire. Un procédé statistique est appliqué aux résultats simulés et une relation empirique est proposée.*

KEYWORDS: *thermally induced seizure, scuffing, oscillating pin-bushing, earthmoving equipment.*

MOTS-CLÉS : *attaque thermiquement induite, éraillure, pion-disque, équipement de terrassement.*

1. Introduction

Heavy-duty earth-moving machinery use linkages that are supported on a pin and bushing pair. A typical schematic of the pin-bushing oscillating pair used in the undercarriage of earth-moving machine is shown in Figure 1. These components generally operate at low-speeds and are subject to very heavy loads. Typically in a pin-bushing pair, the pin is stationary while the bushing oscillates at low frequencies. These pins are typically made of hardened steel and their bushings ID are often treated with a protective coating. Depending on the application, the pin-bushing pair maybe packed with grease during assembly. Some industries use automatic grease feeders and some recommend feeding grease periodically. However, in general, there is no provision for a continuous supply of lubrication in the system and the packed grease is the only source of lubrication. After a period of time of field operation, the pin-bushing pair exhausts the supply of grease packed in the assembly by normal operational leak, wear and tear, and in some instances sealing malfunction. As a result of the inadequate lubrication, the protective bushing coating tends to wear out prematurely and failure occurs as a result of intimate metal-to-metal contact between the pin and the bushing. The mechanism of failure is either scuffing or thermally induced seizure (TIS).

Scuffing is defined as the mode of failure when there is plastic deformation and localized welding of relative moving parts and subsequent wear of the welded parts due to the shear loads. Scuffing failure can occur due to very high stresses and/or a very high rise in temperatures. The combination of heavy loads and high temperatures in oscillating pin-bushing pairs makes them vulnerable to scuffing failure. Thermally Induced Seizure, on the other hand, is the mechanism of failure due to a complete loss in operating clearance in the pin-bushing assembly as the pin encroaches into the bushing.

A significant amount of work has been reported that analyzes the thermomechanical interactions in stationary loaded bearings susceptible to TIS. Bishop and Ettles (1982) analyzed the thermoelastic interaction of a journal in a plastic bushing that was interference-fit with the shaft. A critical *PV/C* number was proposed as an influential parameter for assessing the seizure time. Dufrane and Kannel (1989) analyzed the catastrophic seizure of bearings due to dry friction by a simple one-dimensional equation relating the seizure time to the bearing operating parameters and material properties. Hazlett and Khonsari (1990, 1992) performed a detailed finite element analysis to gain insight into the nature of the contact forces and encroachment of the mating pair leading to TIS of a dry bearing during start up. Wang *et al.* (1996) analyzed the axle burn-off and stack-up force of a railroad roller bearing using the finite element method and independently verified the results of Hazlett and Khonsari's findings. Wang (1997) performed a review of published results on TIS in conformal contacts. It revealed that seizure in unlubricated conformal contacts was primarily due to a thermal ratcheting effect in a positive feedback of increases of interfacial pressure and heat. More recently, Krithivasan and Khonsari (2002, 2003) performed a series of finite element analyses and arrived at a comprehensive equation for predicting TIS in bearings during startup. The majority of published literature is, however, limited to constant, unidirectional operating speeds.

In this paper, the work reported in (Krithivasan and Khonsari, 2003) is extended to include provisions for study of the thermomechanical interaction of heavily loaded pin-bushing assembly in oscillatory motion. The results of an extensive set of FEA results were complied in the form of a useful design equation

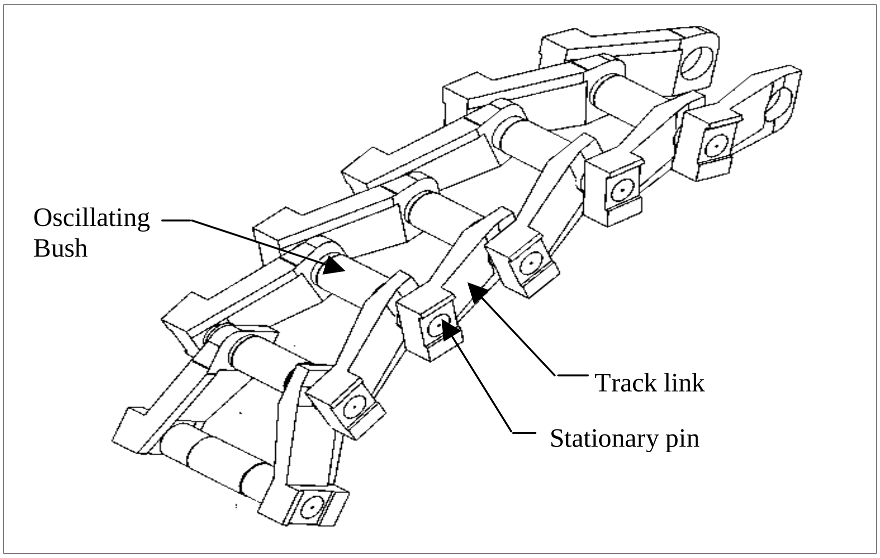

Figure 1. *Track retention assembly with oscillating pin and bushing*

2. Modeling approach

The thermomechanical finite element simulations involved the following a 3-step routine that are explained in detail in Sections 3 through 6.

– Theoretical Hertzian contact analysis;

– Transient finite element thermal analysis using ANSYS 5.7;

– Transient finite element thermomechanical using ANSYS 5.7.

3. Theoretical hertzian contact analysis

The contact area and the contact pressure are calculated from the Hertzian theory of elastic contact. The Hertzian half-contact width for two cylindrical bodies in conformal contact is the following equation (Peterson and Winer, 1980).

$$b = 1.598\sqrt{\frac{WR_{eq}}{LE_{eq}}} \qquad [1]$$

where,

$$R_{eq} = \frac{R_{bi} R_s}{R_{bi} - R_s} \qquad [2]$$

$$E_{eq} = 2\left[\frac{1-\nu_s{}^2}{E_s} + \frac{1-\nu_b{}^2}{E_b}\right]^{-1} \qquad [3]$$

The contact width calculated using Equation [1] is used as a reference to determine the appropriate contact element stiffness in the FE analysis.

4. Transient thermal analysis

The interface frictional heat generated is a function of the contact forces, coefficient of friction and the sliding velocity. Heat is distributed between the pin and the bushing according to the so-called heat partitioning factor, which is dependent on the material properties, thermal mass and the relative velocity of the pin and the bushing. Many commercial FEM software packages can automatically calculate the partition of heat flux. The results of the transient thermal analysis are used in the thermomechanical analysis to determine the pin-bushing interactions.

4.1. *Calculation of heat flux*

The heat flux applied depends on the contact forces, coefficient of friction and the linear velocity. The total heat generated is calculated by the following simple equation.

$$Q = fPv \qquad [4]$$

The heat flux applied is the heat generated applied on the area of contact and is calculated as

$$q_s = \frac{Q}{R_s\, L\, \theta_c} \qquad [5]$$

4.2. *Element types*

The pin and bushing are modeled in ANSYS 5.7 (Ansys Inc., 2001) using the four-noded solid thermal elements viz. PLANE55. This element is compatible with the 4-noded structural solid element used in the thermomechanical analysis.

4.3. *Implementation of oscillating heat flux*

The finite element modeling of the oscillating heat source requires a special formulation. The modeling is done by applying the heat flux as a function of time and space.

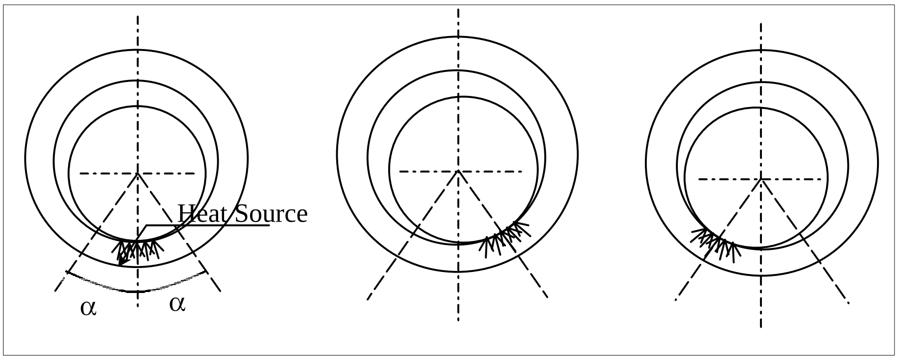

Figure 2. *Schematic of application of oscillating flux, α is the oscillation angle*

The time taken for one complete oscillation (t_{osc}) is calculated from the speed and angle of oscillation. The calculated time for a single oscillation is broken up into a series of *i* time-steps. The calculated flux is applied over a set of elements in the mean position, as shown in Figure 2. The number of elements in contact is calculated from the theoretical Hertzian contact and the element size of the FEA model. The solution is obtained for the first time step i.e. $\delta t = t_{osc}/i$. For the next time sub-step, the flux is moved to the next set of six elements and then solved again for $2\delta t$. This solution is appended to the previous solution. The process is continued until a full oscillation is completed. This sequence is programmed into an ANSYS macro (sub-routine) and repeated cyclically to complete the transient analysis. The application of the flux for the first cycle is illustrated in Figure 3.

4.4. *Boundary conditions for the thermal analysis*

The heat flux, q_s, calculated using Equation [5] is applied on the pin. The temperatures on the pin and the bushing are coupled in the contact region to achieve continuity of temperature in the contact zone. A convective heat transfer coefficient of 30 W/m^2K was applied to the outer surface of the bushing, which is exposed to the ambient. Similarly, a convective heat transfer coefficient was applied to the inner surface between the pin and the bushing where the coefficient is assumed to be a linear function of the surface temperature of the pin and the bushing ID. The value varied from 10 W/m^2K to 35 W/m^2K depending on the surface temperature of the pin and bushing.

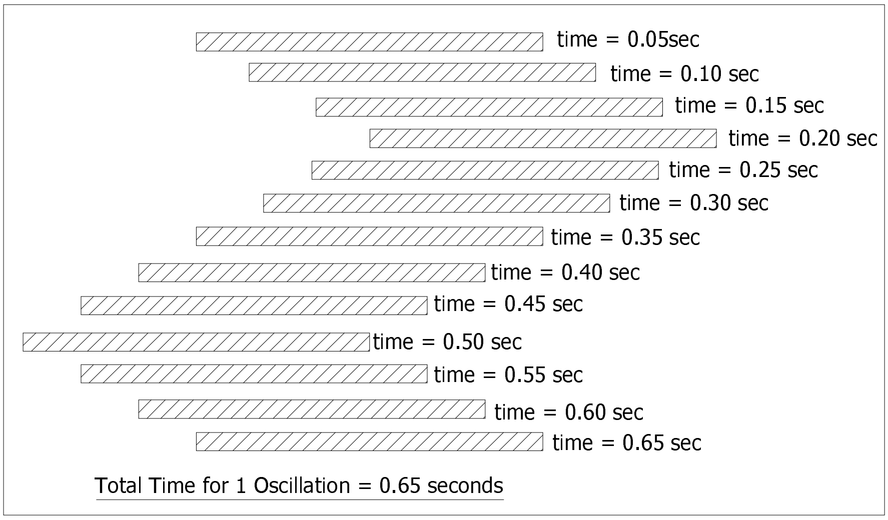

Figure 3. *Application of oscillating heat flux as a function of time and space. In this illustrations, the number of time steps for 1 complete oscillation, i, is 13*

5. Transient thermomechanical analysis

5.1. *Element types*

The solid element PLANE42 is used to model the pin and the bushing. This element is a 2D bilinear element with the x and y displacements as the degrees of freedom. The temperatures obtained from the transient thermal analysis can be applied as nodal loads.

Care needs to be taken when analyzing the radial clearance between the pin and the bushing is. The gap is modeled using 2-noded contact elements CONTAC52 whose schematic is shown in Figure 4. The contact element is activated only when there is a physical contact between the pin and the bushing. Whenever there is contact established between the pin and bushing, the contact element post-processing results give the magnitude of the contact force and negative clearance. The element properties include a normal stiffness value that governs the resistance to normal load. The finite element programmer assigns the stiffness value for the contact element. To determine the appropriate stiffness value, the theoretical Hertzian contact width is found. The stiffness value of the contact element is assigned by trial and error so that the Hertzian contact width and the contact width found by Finite Element method are the same.

5.2. *Meshing*

The meshing pattern is scaled such that the element size is reduced in the radial direction towards the bushing-pin interface as shown in Figure 5. This is done by having coarser elements at the center of the pin and finer elements at the interface. The elements towards the center of the pin degenerate from the standard 4 noded rectangular element into triangles. This methodology is adopted, as our area of interest is the interface of the pin and bushing

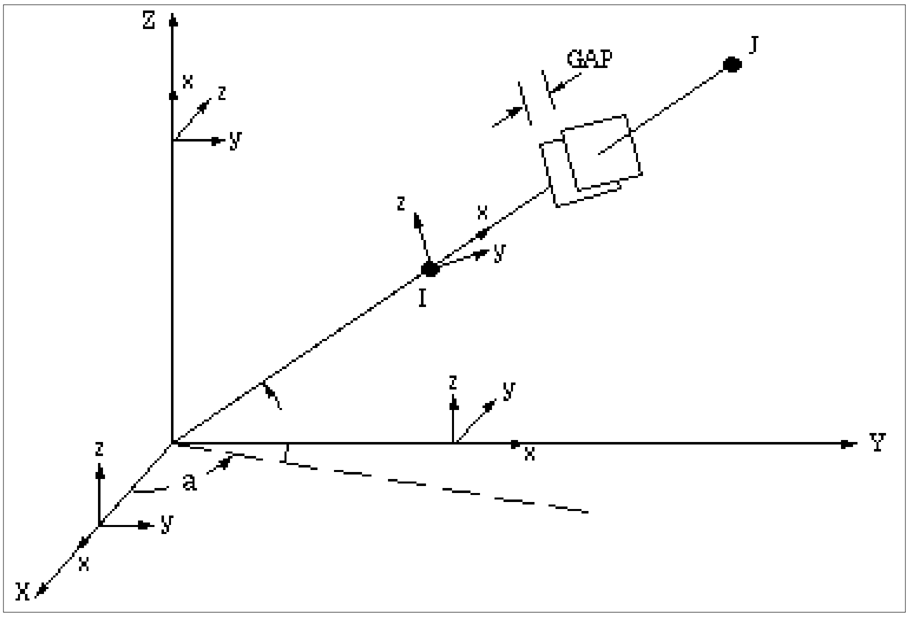

Figure 4. *Schematic of 2-noded contact element connecting nodes "I" and "J"*

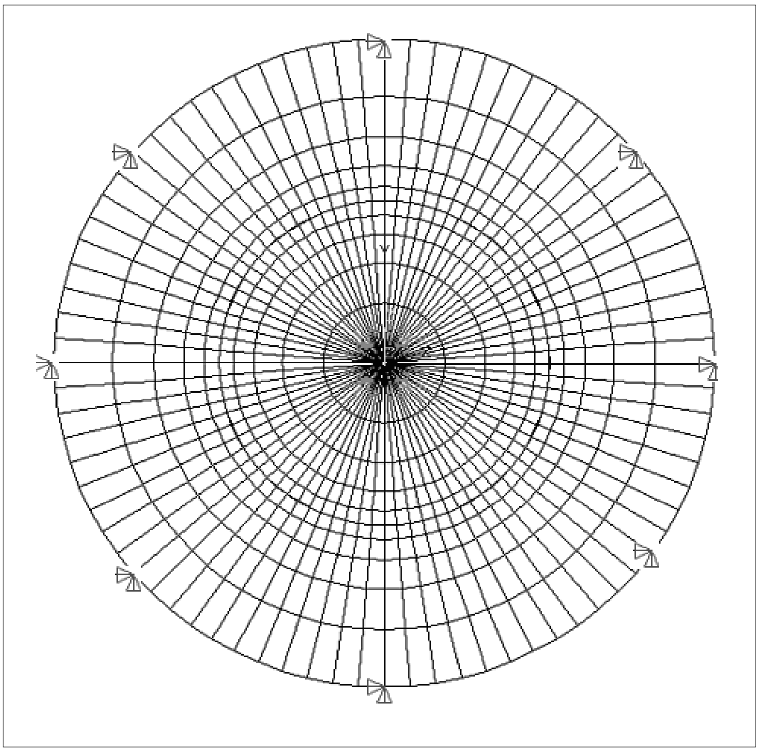

Figure 5. *Mesh pattern for the oscillating pin-bushing assembly*

5.3. *Boundary conditions*

The radial load is applied on the pin on the centerline and the bushing is constrained on the outer diameter as shown in Figure 5. The steady state analysis is performed and the contact element results are analyzed. The transient thermal analysis is followed by the transient thermomechanical analysis to determine the effects of temperature rise on the operating parameters such as operating clearance and the frictional torque. The results of the thermal analysis are applied as thermal nodal loads with respect to time. The radial load acting on the pin is applied as a point force acting on the centerline.

6. Results and discussion

Simulations are performed for a wide range of operating parameters (Table 1). One of the test cases whose operating conditions are given in Table 2 will be used in this section for discussion purposes.

The heat flux as discussed earlier is applied as an oscillating flux with respect to time on the contact region. The oscillating heat flux produces a temperature field as shown in Figure 6, which gives the temperature profile for the first complete oscillation. The temperature profile for the first four time steps shows the effect of flux moving from the mean position to the extreme right position. The maximum temperature also can be seen to move along in the direction of the moving flux. Time steps 4 through 10 give the temperature profile when the heat flux moves from the extreme right position ($+\alpha$ in Figure 2) to the extreme left position ($-\alpha$ in Figure 2). When the flux moves from the extreme right position (Time step #4), it leaves a temperature tail that trails off at the extreme right position ($+\alpha$).

The temperature rise due to the frictional heating causes thermal expansion of the pin and concomitant reduction in operating clearance. The process of loss in clearance in the operating gap between the pin and the bushing is a complex non-linear process. The loss in operating clearance was characterized by an ovalization of the bushing and uniform outward expansion of the shaft, when shafts have unidirectional rotation as explained by Hazlett and Khonsari (1992) and expounded by Krithivasan and Khonsari (2003). The loss in clearance of the oscillating pin-bushing pair is also non-linear because the pin and the bushing are subjected to frictional heating only in the contact region. While the pin has the possibility of thermal expansion outwards, the bushing can only expand inward. The loss in clearance is first observed as the shaft expands and comes in contact with the bushing at the top. This causes new areas to come into contact. This has a two-fold effect, (i) the heat generated has greater area of dissipation between the shaft and the bushing and, (ii) the contact forces and hence the frictional torque increases causing an increase in frictional heat. Figure 7 shows the predicted temperature contours of both the pin and the bushing. It is shown that new areas of contact are created with a simultaneous increase in frictional heat generated. This effect can result in a rapid rise in the contact temperature capable of inducing scuffing failure. The loss in clearance causes the pin to ovalize and come into contact with the bushing at the top of the shaft. This leads to an increased area of contact and subsequent increase in the contact forces. As a result, the frictional heat further contributes to the process of expansion. From the contour profiles in Figure 7, it can be seen that the temperature increases to 752^{o}C after about 6 seconds once ovalization is established. This temperature is sufficient to cause scuffing in steel (Dyson, 1979). Also the frictional torque increased to very high values 6 seconds after ovalization was established.

The failure mode described in this example can be attributed to a combined mode of thermally induced seizure (TIS) and thermal scuffing. Here, the pin-bushing assembly was heavily loaded and the coefficient of friction (and/or the oscillating frequencies) is high. In cases were friction coefficients were low, the maximum temperature reached was about 300-400 ^{o}C and failure occurred by thermally induced seizure (TIS). Typically, lightly loaded assemblies with low coefficients of friction failed by TIS mode while heavily loaded assemblies and material pairs with high coefficients of friction failed by a combination of thermal scuffing and TIS.

Table 1. *Operating parameters for the finite element model and simulations*

Range of pin radii, R_s (m)	35 x 10^{-3} - 75 x 10^{-3}
Range of bearing lengths, L (m)	50 x 10^{-3} - 167 x 10^{-3}
Range of radial clearances, C (m)	0.1 x 10^{-3} - 0.35 x 10^{-3}
Density of pin-bushing ρ (kg/m^3)	1.23 x 10^6
Conductivity, k (W/mK)	54
Thermal expansion coefficient, α (m/mK)	1 x 10^{-5}
Young's modulus of pin-bushing, E (GPa)	200
Poisson's ratio, $\nu_s = \nu_b = \nu$	0.3
Range of loads, W (kN)	66.723- 222.411
Range of friction coefficient, f	0.1 – 0.3
Range of oscillating frequencies, ω_o (rad/s)	1 - 2
Atmospheric Temperature, T_∞ (°C)	25

Table 2. *Operating parameters for the model illustrated for results and analysis*

Pin radius, R_s (m)	0.05
Bearing length, L (m)	0.1
Radial clearance, C (m)	0.25 x 10^{-3}
Coefficient of friction, f	0.3
Oscillating frequency, ω_o (rad/s)	2
Load, W (N)	11205

Verification

The primary reason for failure in the analysis of the pin-bushing assembly is due to the increase in temperature due to frictional heating. The application of proper boundary conditions for the thermal analysis has to be verified to ensure accuracy of the model. A comparison was done between the oscillating thermal analyses done using ANSYS for a one-domain problem with an analytical solution. Krishnamurthy (2002) solved the one-domain oscillating thermal analysis analytically by applying Duhamel's theorem. They also performed dimensional and non-dimensional analysis using another FE solver, FlexPDE (PDE Solutions Inc., 2001). The results of the finite element problems solved using ANSYS and FlexPDE matched closely with the analytical solution. The convergence of the finite element model was also checked using three different mesh sizes.

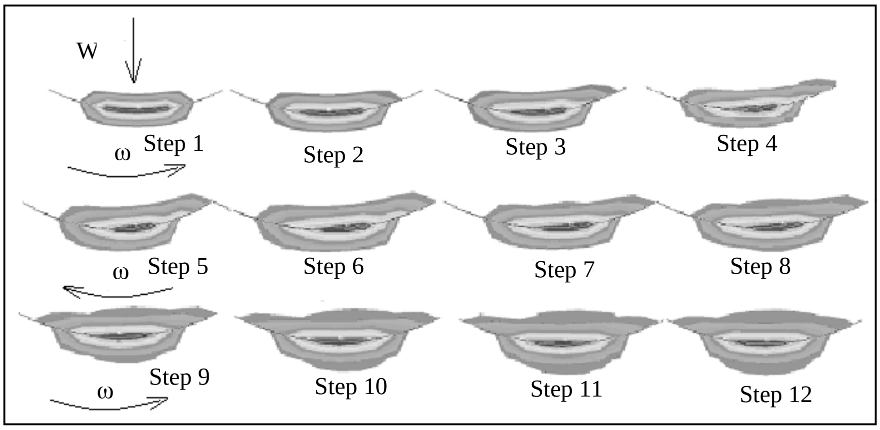

Figure 6. *Temperature contour during 1 cycle of rotation*

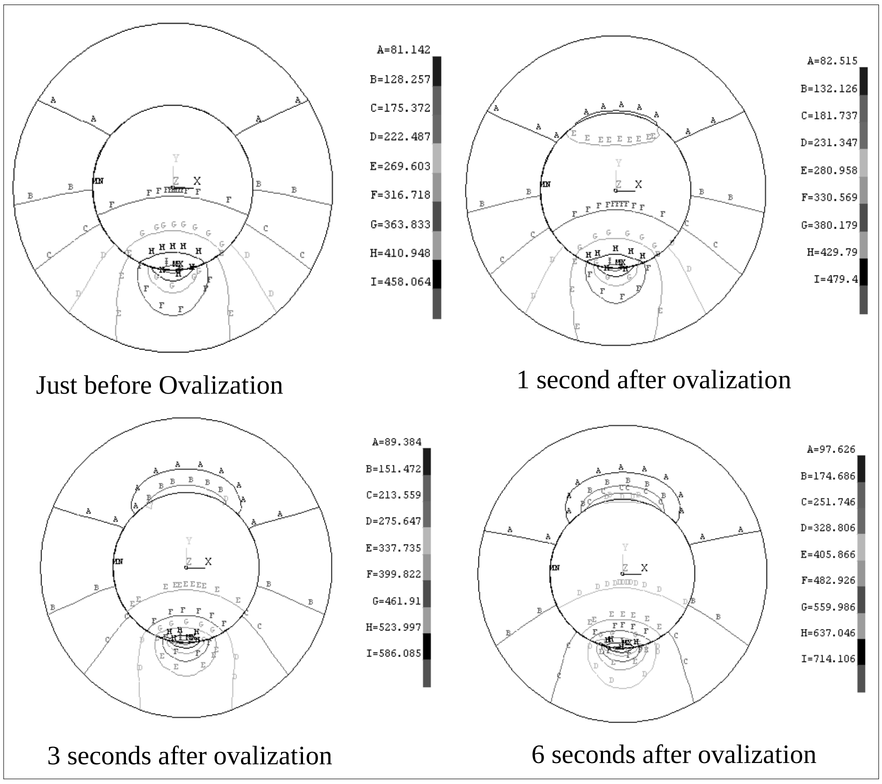

Figure 7. *Temperature contour during failure*

The effect of various operating parameters such as load (*W*), coefficient of friction (*f*) and frequency of oscillation (ω_o) on the failure time is determined by varying the non-dimensional parameter ε. The number of simulations required is thus greatly reduced. The results of varying the various operating parameters are given in Table 3.

The results presented in Table 3 were curve fitted to a goodness value within 98.9%. The expressions relating the thermal strain, aspect ratio and non-dimensional failure time were combined to give Equation 6 for determining the failure time of pin-bushings under oscillating loads.

$$\overline{t}_{fo} = \frac{\varepsilon^{-1.4064}}{2.255\lambda - 70.71} \qquad [6]$$

Table 3. *Variation of failure time at various operating conditions*

<table>
<tr><th>f</th><th>ω_o, (rad/s)</th><th>W (kN)</th><th>R_p, (mm)</th><th>C (mm)</th><th>L (mm)</th><th>t_{fo} (s)</th><th>ε x10^3</th><th>λ</th><th>$\overline{t}_{fo}$</th><th>Temp. at Failure (°C)</th></tr>
<tr><td>0.1</td><td>1</td><td rowspan="8">111.2</td><td rowspan="10">50</td><td rowspan="10">0.25</td><td rowspan="10">100</td><td>6053</td><td>2.139</td><td rowspan="10">100.5</td><td>37.19</td><td>300</td></tr>
<tr><td>0.1</td><td>1.6</td><td>2535</td><td>3.422</td><td>15.58</td><td>322</td></tr>
<tr><td>0.15</td><td>1.2</td><td>2399</td><td>3.849</td><td>14.74</td><td>343</td></tr>
<tr><td>0.2</td><td>1.4</td><td>1488</td><td>5.988</td><td>9.143</td><td>374</td></tr>
<tr><td>0.2</td><td>1.5</td><td>1207</td><td>6.416</td><td>7.416</td><td>380</td></tr>
<tr><td>0.25</td><td>1.6</td><td>936</td><td>8.554</td><td>5.75</td><td>417</td></tr>
<tr><td>0.27</td><td>1.8</td><td>749</td><td>10.97</td><td>4.602</td><td>442</td></tr>
<tr><td>0.3</td><td>2</td><td>582</td><td>12.83</td><td>3.58</td><td>492</td></tr>
<tr><td rowspan="2">0.2</td><td rowspan="2">1.5</td><td>66.72</td><td>3018</td><td>3.849</td><td>18.54</td><td>329</td></tr>
<tr><td>222.4</td><td>564</td><td>12.83</td><td>3.47</td><td>461</td></tr>
<tr><td></td><td></td><td></td><td></td><td></td><td></td><td></td><td></td><td></td><td></td><td></td></tr>
<tr><td rowspan="11">0.2</td><td rowspan="11">1.5</td><td rowspan="11">11120
5</td><td rowspan="6">50</td><td>0.1</td><td rowspan="8">100</td><td>322</td><td rowspan="11">6.416</td><td>250.5</td><td>1.98</td><td>205</td></tr>
<tr><td>0.15</td><td>604</td><td>167.17</td><td>3.71</td><td>265</td></tr>
<tr><td>0.2</td><td>1006</td><td>125.5</td><td>6.18</td><td>314</td></tr>
<tr><td>0.25</td><td>1207</td><td>100.5</td><td>7.42</td><td>380</td></tr>
<tr><td>0.3</td><td>1408</td><td>83.83</td><td>8.65</td><td>440</td></tr>
<tr><td>0.35</td><td>2532</td><td>71.93</td><td>15.56</td><td>465</td></tr>
<tr><td>35</td><td rowspan="5">0.25</td><td>2380</td><td>49.35</td><td>29.84</td><td>405</td></tr>
<tr><td>75</td><td>805</td><td>225.7</td><td>2.20</td><td>446</td></tr>
<tr><td rowspan="3">50</td><td>50</td><td>564</td><td>201</td><td>3.47</td><td>461</td></tr>
<tr><td>100</td><td>1207</td><td>100.5</td><td>7.42</td><td>380</td></tr>
<tr><td>166.7</td><td>2938</td><td>60.3</td><td>18.05</td><td>325</td></tr>
</table>

The following restrictions apply to equation [6].

– The finite element was limited to a 2-dimensional analysis, assuming that the contact pressure is uniform across the bearing length and there is no misalignment of the shaft in the bearing. The material properties were assumed to be constant and the analysis did not consider elastic deformation;

– The time for failure as given in Equation [6] gives the approximate failure time (t_{fo}) after there is complete loss of initial lubrication in the pin-bush assembly and loss of anti-friction coating;

– Equation [6] gives the failure time for pin-bush assembly when there is continuous oscillating motion. But in practice, there is only intermittent loads acting on the pin-bushing assembly. The time to failure predicted is for the worst-case scenario. To obtain a practical failure time, the loading cycle of the oscillating pin-bushing has to be incorporated with Equation [6];

– The Hertzian contact pressure in the contact region is parabolic and hence the frictional heat flux is also a parabolic function. But a constant heat flux is applied in the thermal analysis for simplicity;

– The oscillating frequency, ω_o, is assumed to be constant for small intervals of time.

7. Summary and concluding remarks

The analysis of a heavily loaded pin-bushing assembly subject to oscillating loading was analyzed using finite element thermal analysis and thermomechanical analysis. The reasons for bearing failure were analyzed by performing simulations for different types of operating conditions. It was found that failure of these pin-bushings occurred by thermally induced seizure for lighter boundary conditions and by a combination of TIS and thermal galling for more severe boundary conditions. The time for failure in the non-dimensional form was derived from a series of simulations and is given by the following equation.

$$\overline{t}_{fo} = \frac{\varepsilon^{-1.4064}}{2.255\lambda - 70.71}$$

This paper was performed as a preparatory work for a grant supported in part by the Louisiana Board of Regents (LEQSF-(2002-05)-RD-B-03) through an industrial ties research program with Caterpillar Inc. The authors greatly acknowledge the sponsors' financial support and encouragement.

8. References

ANSYS Inc., ANSYS 5.7 Online Users Manual, 2001, ANSYS Inc.

Bishop J.L., McC. Ettles C.M., "The seizure of journal bearings by thermoelastic mechanisms", *Wear*, Vol. 79, 1982, pp. 37-52.

Dufrane K., Kannel J., "Thermally induced seizures of journal bearings", *ASME Journal of Tribology*, Vol. 111, 1989, pp. 288-292.

Dyson A., "Scuffing", *Treatise on Material Science and Technology*, Vol. 13, 1979, pp. 175-215.

Hazlett T.L., Khonsari M.M., "Finite element model of journal bearing undergoing rapid thermally induced seizure", *Tribology International*, Vol. 25, No. 3, 1992a, pp. 177-182.

Hazlett T.L., Thermoelastic behavior of journal bearing undergoing seizure – a finite element study, M.S. Thesis, University of Pittsburgh, Pittsburgh, Pennsylvania, 1990.

Krishnamurthy H., Application of Duhamel's Theorem to Problems Involving Oscillating Heat Source, M. S. Thesis, Department of Mech. Engr., Louisiana State University, 2002.

Krithivasan R., Khonsari M.M., "Thermally Induced Seizure in Journal Bearings during Startup and Transient Flow Disturbance", *ASME Journal of Tribology*, Vol. 125, 2003, pp. 833-841.

Krithivasan R., Transient Thermomechanical Interactions of Shaft- Bushing Pair in Bearings – A Finite Element Study, M.S. Thesis, Department of Mechanical Engineering, Louisiana State University, 2002.

PDE Solutions Inc., FlexPDE: A Flexible Solution for Partial Differential Equations Version 2.20e 3D Online Reference Manuals, 1996-2001, PDE Solutions Inc.

Peterson M.B., Winer W.O., "Wear Control Handbook", *ASME*, 1980, pp. 115.

Wang H., Axle Burn-off and Stack-up Force Analyses of a Railroad Roller Bearing using the Finite Element Method, Ph.D. Thesis, Department of Mechanical and Industrial Engineering, University of Illinois at Urbana-Champaign, 1996, 35, pp. 140-147.

Wang H., Conry T.F., Cusano C., "Effects of Cone/Axle Rubbing Due to Roller Bearing Seizure on the Thermomechanical Behavior of a Railroad Axle", *ASME Journal of Tribology*, Vol. 118, 1996, pp. 311-319.

Wang Q., "Seizure Failure of journal-bearing conformal contacts", *Wear*, Vol. 210, 1997, pp. 8-16.

9. Nomenclature

A_s	=	Area of the shaft that is in contact with the bushing, m^2
b	=	Semi contact width, m
C	=	Radial clearance, m
C_p	=	Specific heat capacity, J/kgK
E	=	Young's modulus, N/m^2
E_{eq}	=	Equivalent modulus of elasticity, N/m^2
f	=	Coefficient of friction
i	=	Number of time steps to complete 1 complete oscillation
k	=	Thermal conductivity, W/mK
L	=	Length of the bearing in the normal direction, m

n	=	Heat partition factor
P	=	Contact force between the journal and the bearing, N
q_s	=	Heat flux entering the shaft, W/m^2
Q	=	Heat generated, W
R_{bi}	=	Inside radius of the bushing, m
R_{bo}	=	Outer radius of the bushing, m
R_s	=	Radius of the journal, m
R_{eq}	=	Equivalent radius of contact, m
t_{fo}	=	Failure time for oscillating pin-bushing, seconds
$\overline{t}_{fo}$	=	Non-dimensional failure time for oscillating pin-bushing
t_{osc}	=	Time for one complete oscillation, seconds
u	=	Surface velocity of the journal, m/s
W	=	Load acting on the shaft, N
α	=	Coefficient of thermal expansion, m/mK
ε	=	Non-dimensional thermal strain
κ	=	Thermal diffusivity, m^2/s
λ	=	Non-dimensional modified aspect ratio
ν	=	Poisson's ratio
ρ	=	Density of the material, kg/m^3
θ_c	=	Contact angle, radians
ω_o	=	Oscillating frequency, radians/seconds

Subscripts

s	=	Shaft or Journal or Pin
b	=	Bushing